# On the origin of the late-side tail in the time-of-flight distribution: A long-standing puzzle solved

Brennan Schaefer, Oak Ridge National Laboratory

Herein we derive from first principles the distribution of flight times for particles of a specified momentum range. A preliminary model is used for illustration that assumes a fixed path length, and later refinements more closely describe particles produced in high energy collisions traversing an orthogonal magnetic field in a cylindrical detector. The time of flight distribution as a whole is shown to descend directly from momentum uncertainty, timing uncertainty, and detector geometry.

## Introduction

Time of Flight (TOF) techniques are used in many fields for a very diverse range of purposes including: neutron kinetic energy measurements for crystallography [1], TOF mass spectrometry [2], topographical imaging [3], TOF in positron emission tomography [4], and particle identification for high energy collision detectors [5]. The mathematical methods used in this work are readily transferable to other TOF applications.

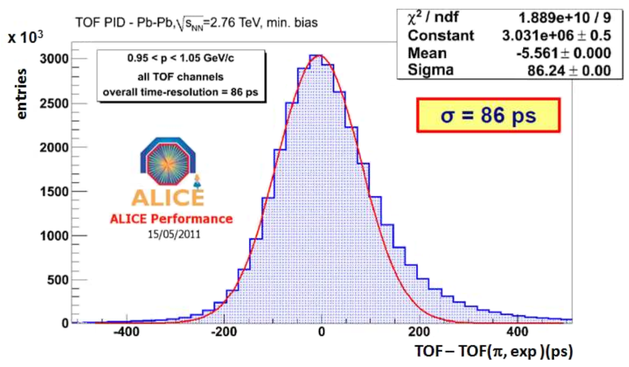


ALICE performance plot showing a time of flight distribution normalized to the time expected for pions. Early arrival (left side) is well approximated by a Gaussian fitting function, and the late arrival tail departs significantly [6].

TOF detectors are used for particle identification in high energy collision experiments (ALICE, HADES, PHENIX, PHOBOS and STAR, and planned for BESIII, MPD at JINR and SoLID at JLab). Particle velocities are found from their time of flight and reconstructed path lengths, and species are separated according to their velocities.

## Key Questions

- What gives rise to the asymmetry in the Time of Flight detector response?
- Does the pronounced late-side tail constitute part of the signal or background?

A number of explanations have been put forward in publications and colloquially to explain the TOF response asymmetry, including:

- Particle species contamination
- Feed-down contamination
- Inner-outer track mismatches / detector bias
- Multiple scattering energy loss

At low $p_T$ particle species separation can exceed 99% purity, discounting contamination. Kaon timing peaks exhibit similar proportioned late-side tails while having far less feed-down than pion and proton peaks, discounting the feed-down explanation. Track matching refinements only improve the TOF peak widths to a point and subsequently do not reduce the late-side tail, possibly discounting the track matching explanation.

Both PHENIX and ALICE feature similarly proportioned late-side tails despite having widely varied material budgets, discounting the multiple scattering explanation.

## Explanation

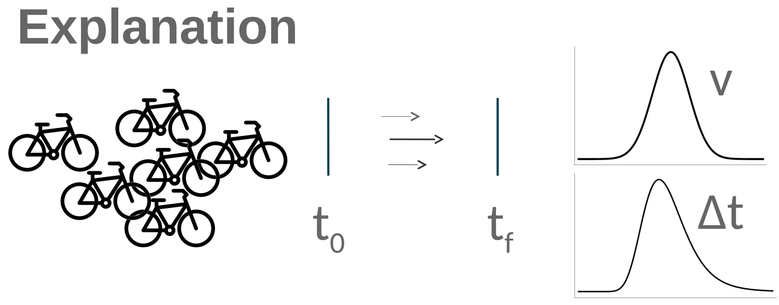


A Gaussian distribution of velocities (relativistic or otherwise) will necessarily correspond to an asymmetric distribution of crossing times over a fixed distance.

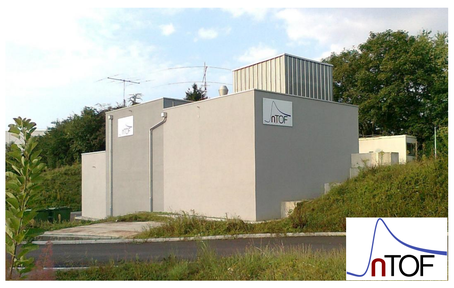


The Neutron TOF experiment at CERN uses a spallation source and reconstructs kinetic energy for cross section measurements.

Using narrow transverse momentum selection intervals, the $p_T$ uncertainty may be approximated as Gaussian.

The corresponding distribution of velocities and TOF for a given mass and over a fixed distance are derived as follows.

$$P(p) = \frac{A}{\sqrt{2\pi\sigma^2}}\, e^{-\frac{(p-\mu)^2}{2\sigma^2}}$$

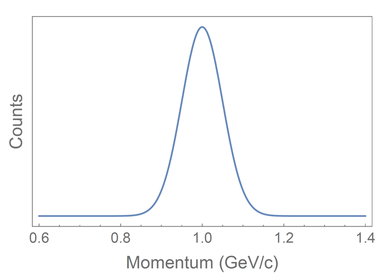


Requiring only that the areas of both distributions are equal:

$$\int_{v_1}^{v_2} V(v)\, dv = \int_{p_1}^{p_2} P(p)\, dp$$

$$p = mv\gamma = \frac{mv}{\sqrt{1-\frac{v^2}{c^2}}}$$

$$\int_{v_1}^{v_2} V(v)\, dv = \int_{v_1}^{v_2} \frac{A}{\sqrt{2\pi\sigma^2}}\, e^{-\frac{(mv\gamma-\mu)^2}{2\sigma^2}} \left(\frac{dp}{dv}\right) dv$$

$$\int_{v_1}^{v_2} V(v)\, dv = \int_{v_1}^{v_2} \frac{A}{\sqrt{2\pi\sigma^2}}\, e^{-\frac{(mv\gamma-\mu)^2}{2\sigma^2}} \left(\frac{m}{\gamma^3}\right) dv$$

$$V(v) = \frac{A}{\sqrt{2\pi\sigma^2}}\, \frac{m}{\gamma^3}\, e^{-\frac{(mv\gamma-\mu)^2}{2\sigma^2}}$$

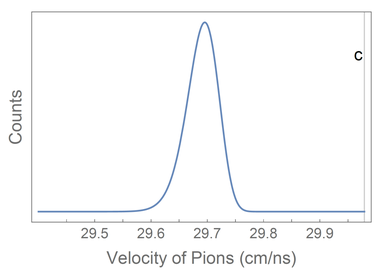


The same procedure used to map into T(t) space gives:

$$T(t) = \frac{A}{\sqrt{2\pi\sigma^2}}\, \frac{mc^3 d}{t^2\left(c^2-\frac{d^2}{t^2}\right)^{\frac{3}{2}}}\, e^{\frac{-\left(\frac{mcd}{\sqrt{t^2c^2-d^2}}-\mu\right)^2}{2\sigma^2}}$$

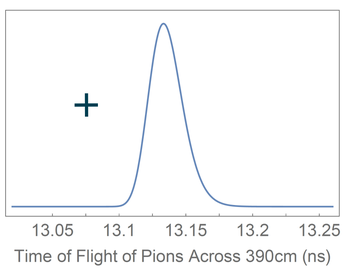


## Refinements

In a cylindrical detector geometry and orthogonal magnetic field the path length corresponding to $p_T + dp_T$ is shorter than that for $p_T - dp_T$, thus enhancing the late and early tails.

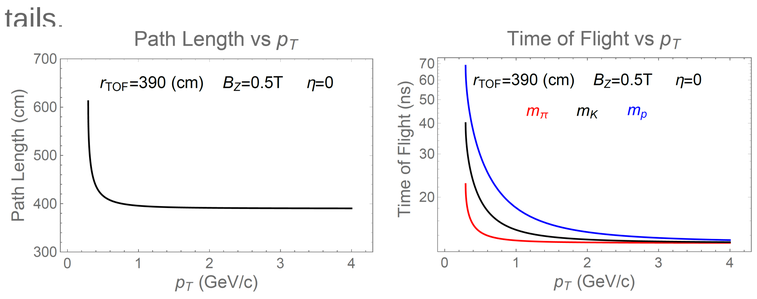


The $p_T$ distribution can alternately be mapped from the Lagrange inverse of the following relation found using kinematics and boundary conditions:

$$t_{TOF} = \frac{2\sqrt{m^2 + p_T^2\cosh^2(\eta)/c^2}}{qB_z} \arcsin\left(\frac{q\,B_z\,r_{TOF}}{2p_T}\right)$$

At low $p_T$ the influence of the variable path length is high.

A more realistic $p_T$ uncertainty distribution can be found from fit-to-data and adding the uncertainty with convolution.

$$\widetilde{P}_T(x) = e^{a+bx}\,\Theta(x-\alpha)\,\Theta(\beta-x)$$

$$\xi_{p_T}(p_T) = \frac{1}{\sqrt{2\pi\sigma^2}}\, e^{-\frac{(p_T-\mu)^2}{2\sigma^2}}$$

$$P_T(p_T) = \int_{-\infty}^{\infty} \widetilde{P}(x)\xi_{p_T}(p_T-x)\,dx = \int_{\alpha}^{\beta} e^{a+bx}\,\frac{1}{\sqrt{2\pi\sigma^2}}\, e^{-\frac{(p_T-x-\mu)^2}{2\sigma^2}}\,dx$$

$$P_T(p_T) = \frac{e^{-b(p_T-\mu)+\frac{b^2\sigma^2}{2}}}{2}\left(Erf\left(\frac{-p_T+\beta+\mu+b\sigma^2}{\sqrt{2}\sigma}\right) - Erf\left(\frac{-p_T+\alpha+\mu+b\sigma^2}{\sqrt{2}\sigma}\right)\right)$$

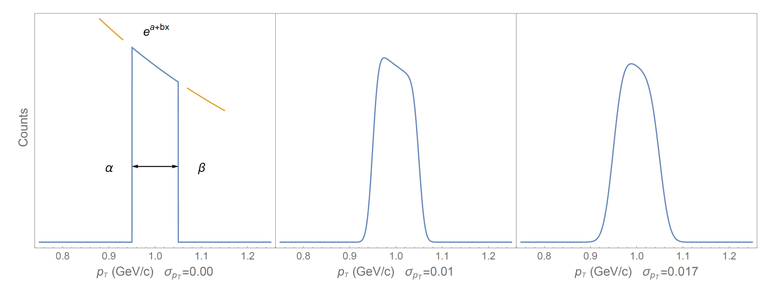


After mapping into T(t) space, a second convolution can be used to yield T (t) which includes timing uncertainty [7].

## Conclusions

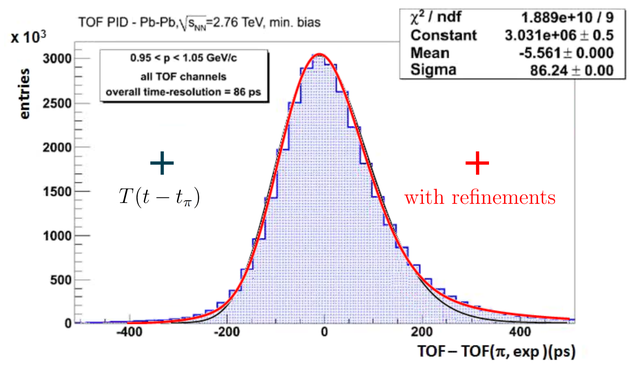


- The asymmetric TOF(t) distribution is the product of uncertainty in timing and momentum, and detector geometry.
- The late-side tail constitutes part of the signal and consequently the mean is to the right of the apparent Gaussian mean.

## References

**1.** Rev. of Sci. Instr. 82, 204 (2011)
**2.** Instr. of Sci. & Tech.16, 1-14 (1987)
**3.** *TOF Cameras: Prin.Meth&Apps* Springer (2012)
**4.** J. of Instr. 9, C10030, (2014).
**5.** NIM 593, 307-313 (2008).
**6.** NIM 706, 29-32 (2013)
**7.** Schaefer, Loizides in prep 2018